AIP Journal of Applied Physics

Theoretical investigation on the existence of inverse and direct magnetocaloric effect in perovskite EuZrO3

B. P. Alho, E. P. Nóbrega, V. S. R. de Sousa, A. Magnus G. Carvalho, N. A. de Oliveira, and P. J. von Ranke

Citation: Journal of Applied Physics **109**, 083942 (2011); doi: 10.1063/1.3582144
View online: http://dx.doi.org/10.1063/1.3582144
View Table of Contents: http://scitation.aip.org/content/aip/journal/jap/109/8?ver=pdfcov
Published by the AIP Publishing

Theoretical investigation on the existence of inverse and direct magnetocaloric effect in perovskite $EuZrO_3$

B. P. Alho,[1,a)] E. P. Nóbrega,[1] V. S. R. de Sousa,[1,2] A. Magnus G. Carvalho,[3] N. A. de Oliveira,[1] and P. J. von Ranke[1]
[1]*Instituto de Física, Universidade do Estado do Rio de Janeiro - UERJ, Rua São Francisco Xavier, 524, 20550-013, RJ, Brazil*
[2]*Instituto de Física Gleb Wataghin, Universidade Estadual de Campinas - UNICAMP, 13083-970, Campinas, SP, Brazil*
[3]*Divisão de Metrologia de Materiais (DIMAT), Instituto Nacional de Metrologia, Normalização e Qualidade Industrial (INMETRO), Duque de Caxias, RJ, 25250-020, Brazil*

(Received 13 December 2010; accepted 28 March 2011; published online 29 April 2011)

We report on the magnetic and magnetocaloric effect calculations in antiferromagnetic perovskite-type $EuZrO_3$. The theoretical investigation was carried out using a model Hamiltonian including the exchange interactions between nearest-neighbor and next-nearest-neighbor for the antiferromagnetic ideal G-type structure (the tolerance factor for $EuZrO_3$ is $t = 0.983$, which characterizes a small deformation from an ideal cubic perovskite). The molecular field approximation and Monte Carlo simulation were considered and compared. The calculated magnetic susceptibility is in good agreement with the available experimental data. For a magnetic field change from zero to 2 T a normal magnetocaloric effect was calculated and for a magnetic field change from zero to 1 T, an inverse magnetocaloric effect was predicted to occur below T = 3.6 K. © *2011 American Institute of Physics*. [doi:10.1063/1.3582144]

I. INTRODUCTION

The magnetocaloric effect (MCE) is observed when a magnetic sample presents temperature changes upon variation of the external magnetic field and is usually described by ΔS_T (the isothermal magnetic entropy change) and ΔT_{ad} (the adiabatic temperature change). The MCE was discovered by Warburg[1] in 1881. In the last thirteen years, interest in the MCE was strongly renewed due to the discovery of the first giant magnetocaloric material reported by Pecharsky and Gschneidner,[2] and to the possibility of its application in room temperature magnetic refrigeration. Besides the technological interest, the MCE shows great potential for the investigation of the fundamental physical properties of magnetic materials, since the origin of the MCE is due to the link between the crystal lattice and the magnetic lattice. For example, the magneto-elastic coupling,[3] the nature of the first and second order magnetic and crystalline phase transitions,[4] the crystalline electrical field magnetic anisotropy,[5] the charge-ordering contribution to the heat capacity and entropy change,[6] spin fluctuations[7] and the magnetic disorder problems[8] have already been addressed in the literature. The large experimental database for several kinds of magnetic materials and the theoretical aspects of the MCE was reported in Refs. 9 and 10).

The perovskite oxides include insulators, semiconductors, and systems with metallic, magnetic, and superconducting behavior, exhibiting an enormous variety of physical phenomena and are important in numerous technological areas. An ideal cubic perovskite has the formula ABO_3, in which the B ion is surrounded by an octahedron of oxygen atoms and the A ion is surrounded by twelve oxygen atoms, as shown in Fig. 1. The structural deformation from an ideal cubic perovskite is primarily determined by the size-ratio of the two kinds of ions occupying A and B sites. The cubic distortion can be quantified by the tolerance factor, $t = \langle A - O\rangle / \sqrt{2}\langle B - O\rangle$, where $\langle A - O\rangle$ and $\langle B - O\rangle$ are the mean atomic distances between the A ion and oxygen and the B ion and oxygen, respectively. For an ideal cubic perovskite, $t = 1$.[11] There are a few works about the MCE in materials with a perovskite-like structure. Kuz'min and Tishin[12] investigated the MCE in the perovskite structural compounds $RAlO_3$, where (R = Gd, Dy, Er, and Yb) and compared them with the garnets, $Dy_3Al_5O_{12}$ and $R_3Ga_5O_{12}$ (R = Gd, Dy). They concluded by theoretical analysis that these perovskite compounds are better refrigerants than the garnets in the temperature range from 4.2 to 20 K. Kimura *et al.*[13] showed that ΔS_T, calculated through magnetic measurements in single crystals of $RAlO_3$, where (R = Dy, and Er) are larger than $Dy_3Al_5O_{12}$ and $Dy_3Ga_5O_{12}$, is in agreement with the calculation by Kuz'min and Tishin. The MCE in ferromagnetic perovskite manganites $R_{1-x}M_xMnO_3$ (R = La, Nd, Pr and M = Ca, Sr, Ba, etc.) was thoroughly investigated and Phan and Yu[14] published a review of these materials, highlighting the nature of their magnetocaloric properties and potentials for magnetic refrigeration application.

Recently, Zong et *al.*[15] investigated the crystal structure and magnetic susceptibility of polycrystalline $EuZrO_3$. Through Rietveld analysis of the x-ray diffraction patterns, the orthorhombic perovskite-type structure was determined, leading to the tolerance factor, $t = 0.983$. Through the susceptibility measurement, an antiferromagnetic order was observed below T = 4.1 K. Using the values of the exchange

a)Author to whom correspondence should be addressed. Electronic mail: brunoalho@gmail.com. Telephone and Fax: 0055 21 23340575.

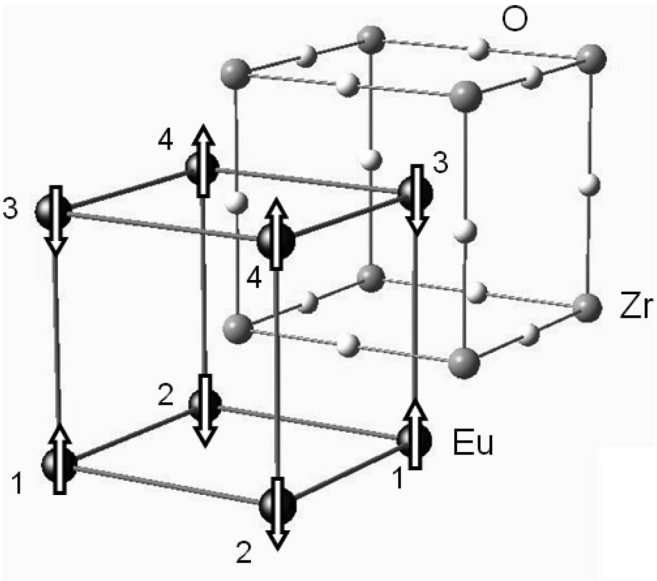

FIG. 1. Schematic representation of the G-type antiferromagnetic crystal structure for $EuZrO_3$, where the numbers localize the four different magnetic sites.

parameters obtained by Zong *et al.*,[15] Kolodiazhnyi *et al.*[16] calculated the spin pair correlation function between nearest-neighbors Eu^{+2} in $EuZrO_3$ and investigated the magnetodielectric effect. They concluded that the magnetodielectric coupling in $EuZrO_3$ is much smaller than that observed in $EuTiO_3$.

In the present work, we focus on the magnetic and MCE properties of $EuZrO_3$. As reported by Zong *et al.*,[15] the Eu^{+2} valence state is dominant ($n=0.96$) compared with the Eu^{+3} state ($n=0.04$) and the tolerance factor is close to one. Therefore, we considered a four-magnetic-lattice Hamiltonian, in which the Eu^{+2} ions in $EuZrO_3$ are localized in the corner of a simple cube, without the crystalline electrical field interaction (since Eu^{+2} is an S-state). From our model Hamiltonian, in the mean field approximation (MFA), four coupled magnetic state equations were obtained and, from the self-consistent solution, the magnetization, susceptibility, ΔS_T, and ΔT_{ad} were calculated. Additionally, these magnetic and thermodynamic quantities were simulated using the Monte Carlo (MC) procedure. Our theoretical results for the magnetic susceptibility are in good agreement with the Zong *et al.* experimental data in both the antiferromagnetic and paramagnetic phases. The predicted change in the MCE, from normal-MCE to an inverse MCE, highlights the spin-flip in $EuZrO_3$ under a magnetic field of about 1 T, at T = 2 K.

II. THEORY

A. Generalized Mean Field

The generalized mean field theory is usually applied for magnetic systems described by two or more magnetic sublattices, including next or more distant nearest-neighbor exchange interactions. In the case of $EuZrO_3$, we considered four distinct magnetic sublattices indicated in Fig. 1 by the numbers (1), (2), (3) and (4). The crystalline electrical field is neglected, since the Eu^{+2} – magnetic ions present the S-state. The model Hamiltonian includes the exchange and Zeeman interactions

$$H = -\sum_{l,m} J_{l,m} S_l . S_m - g\mu_B B \sum_l S_l, \tag{1}$$

where $J_{l,m}$ is the exchange parameter, S_l and S_m are spin operators for the magnetic ions at l and m-sites, g is the Landé-factor (in the present case, $g=2$), μ_B is the Bohr magneton, and B is the applied magnetic field. Under the mean field approximation, the Hamiltonian (1) reads

$$H = -g\mu_B \sum_{l=1}^{n} B_l^{\text{eff}} S_l, \tag{2}$$

where

$$B_l^{\text{eff}} = B + \sum_{m=1}^{n} \gamma_{lm} M_m, \tag{3}$$

and

$$\gamma_{lm} = \frac{2nZ_{l,m}J_{l,m}}{g^2\mu_B^2 N}. \tag{4}$$

Here, B_l^{eff} is the effective field acting on the l-ion, N is the number of magnetic ions per volume, n is the number of magnetic sublattices (in the present case, $n=4$) and $Z_{l,m}$ is the number of m neighbors of an l- ion. For example, from Fig. 1, the effective field at site (1) is given by $B_1^{\text{eff}} = B + 4J_2M_1 + 4J_1M_2 + 2J_1M_3 + 8J_2M_4$, where J_1 and J_2 are the nearest and next-nearest-neighbors effective exchange interaction parameters, respectively. The magnetization of the l-sublattice is given by

$$M_l = \frac{gS\mu_B N}{n} B_S\left(\frac{gS\mu_B B_l^{\text{eff}}}{k_B T}\right), \tag{5}$$

where $S=7/2$ is the total spin of the Eu^{+2} ion, k_B is the Boltzmann constant, and B_S is the Brillouin function. Since $l=1$, 2, 3, and 4, the calculation of the magnetic state equation (5) requires a numerical self-consistent solution of the four coupled equations, where an initial value, M_l^0, is given for the magnetization of each sublattice and M_l is calculated. Then, this value is inserted again in relation (5), substituting M_l^0. This process is repeated until $M_l = M_l^0$. To locate the transition temperatures in agreement with the generalized mean field theory, we set $B=0$ in the high temperature approximation, which leads to a linear homogeneous set of equations in relation (5). Under the condition to a have nonzero solution for M_l, four solutions emerge for the critical temperatures, corresponding to the possible magnetic arrangements (one ferromagnetic, F, and three antiferromagnetic types, namely: A, C, G).[17] As concerns the $EuZrO_3$, we are interested in a G-type antiferromagnetic spin arrangement (see Fig. 1) as pointed out by Zong *et al.*,[15] for which the antiferromagnetic-paramagnetic critical temperature is given by

$$T_N^{G-type} = \frac{2S(S+1)}{3k_B}(-6J_1 + 12J_2). \tag{6}$$

The main contributions to the total entropy, $S(T,B)$, in $EuZrO_3$ include the lattice and magnetic entropies

$$S(T,B) = S_{\text{latt}}(T) + \frac{R}{n}\sum_{l=1}^{n}\left[\ln(Z_l) - \left(\frac{gS\mu_B B_l^{\text{eff}}}{k_B T}\right)B_S\left(\frac{gS\mu_B B_l^{\text{eff}}}{k_B T}\right)\right], \quad (7)$$

where

$$Z_l = \sinh\left[\frac{2S+1}{2S}\left(\frac{gS\mu_B B_l^{\text{eff}}}{k_B T}\right)\right] \Big/ \sinh\left[\frac{1}{2S}\left(\frac{gS\mu_B B_l^{\text{eff}}}{k_B T}\right)\right], \quad (8)$$

and

$$S_{\text{latt}}(T) = N_a R\left[-3\ln(1-e^{-\Theta_D/T}) + 12\left(\frac{T}{\Theta_D}\right)^3\int_0^{\Theta_D/T}\frac{x^3}{e^x-1}dx\right]. \quad (9)$$

Here $N_a = 5$ is the number of atoms per unit formula, R is the gas constant, and Θ_D is the Debye temperature.

The magnetocaloric quantities, ΔS_T and ΔT_{ad}, in the MFA were obtained directly from the total curves of entropy versus temperature [relation (7)], with and without applied magnetic field.

B. Monte Carlo Method

For an alternative description of the thermodynamic properties along with the magnetocaloric effect in $EuZrO_3$, the spin Hamiltonian (1) is also treated in the classical Monte Carlo simulation.[18,19] Different from the MFA, the MC simulation includes the short range interactions, which are important around the temperature of magnetic phase transition.

The classical Monte Carlo simulation for the Heisenberg Hamiltonian does not provide the saturation value of the magnetic entropy, $S_{\text{mag}} = R\ln(2S+1)$, where the term $(2S+1)$ gives the number of accessible states, because the spins are treated as classical variables that can assume a continuous range of values. Therefore, in order to reproduce the expected saturation value of the magnetic entropy, the Potts-like model was used,[20] where the azimuthal components of the spins were considered as quantum quantities, which can only assume discrete values in the interval, $-S \le S^z \le +S$.

In order to calculate the mean energy, $\langle H\rangle$, for a given temperature, the Metropolis algorithm was used.[18] For a Monte Carlo step, the energy of the system is the energy of the last generated spin configuration, (E_i), where the label 'i' represents the number of a given Monte Carlo step. The mean energy, $\langle H\rangle$, is calculated by

$$\langle H\rangle = \frac{1}{N_C - N_0}\sum_{i=N_0+1}^{N_C} E_i, \quad (10)$$

where N_C represents the total number of Monte Carlo steps and N_0 is the number of Monte Carlo steps used for thermalization of the system. The mean square energy, $\langle H^2\rangle$, was obtained by a relation analogous to Eq. (10). At a given temperature, the average magnetization per Eu^{+2} ion was calculated by the relation $M/\text{ion} = g\mu_B\langle S\rangle$, where the mean value of the spin angular momentum, for each lattice site is given by

$$\langle S\rangle = \frac{1}{N_C - N_0}\sum_{i=N_0+1}^{N_C}\left(\frac{1}{N_S}\sum_{K=1}^{N_S} S_K\right), \quad (11)$$

where the label 'i' represents the Monte Carlo cycle, the label 'K' represents the lattice sites, and N_S represents the number of lattice sites. The magnetic contribution to the heat capacity and to the magnetic susceptibility at a fixed temperature were calculated by the usual relations

$$C_{\text{mag}}(T,B) = \frac{\langle H^2\rangle - \langle H\rangle^2}{k_B T^2} \quad (12)$$

and

$$\chi(T,B) = \frac{\langle M^2\rangle - \langle M\rangle^2}{k_B T}. \quad (13)$$

In order to calculate the physical quantities of interest to study the magnetocaloric effect in $EuZrO_3$, we used a three-dimensional cluster of $5\times5\times5$ cubic unit cells with four Eu^{+2} ions per cell, considering the nearest and next-nearest neighbors interactions. The Monte Carlo simulation was performed using 50 000 Monte Carlo steps, where 25 000 were used for thermalization of the system and 25 000 were used to compute the average values of the physical quantities at each temperature. The mean values of the energy and spin were calculated from relations (10) and (11). The magnetic contribution to the heat capacity and magnetic susceptibility were calculated using relations (12) and (13). The magnetic entropy was calculated by integration of the heat capacity curve over the entire temperature range using the relation, $S = \int (C/T\prime)dT\prime$. The lattice entropy was considered in the Debye assumptions [see relation (9)]. The magnetocaloric quantities, ΔS_T and ΔT_{ad}, were obtained in the same way as that discussed in the mean field calculations.

III. RESULTS AND DISCUSSIONS

The temperature dependence of the magnetization in $EuZrO_3$ is shown in Fig. 2 for applied magnetic fields $B = 0.005$, 0.01, and 0.02 T. The solid lines are the results from the MFA and the symbols represent the results of the MC simulations. In the mean field model, the effective exchange parameters used were $J_1/k_B = -0.032$ K and $J_2/k_B = +0.017$ K. These values reproduce the measured Néel temperature $T_N^{G-\text{type}} \sim 4.16$ K (see relation 6) of $EuZrO_3$.[15] The exchange interaction parameters for nearest and next-nearest neighbors interactions in $EuZrO_3$, used in the Monte Carlo simulation, were $J_1^{\text{MC}} = -0.0056$ meV $(-0.065$ K) and $J_2^{\text{MC}} = 0.0043$ meV (0.05 K), respectively. These parameters were chosen to correctly reproduce the experimental order temperature. Despite the large difference between the mean field approach and the Monte Carlo procedure to deal with the model Hamiltonian, relation (1), the obtained exchange parameters sets $[J_1, J_2]$ and $[J_1^{\text{MC}}, J_2^{\text{MC}}]$ are within the same order of magnitude. The profiles of M

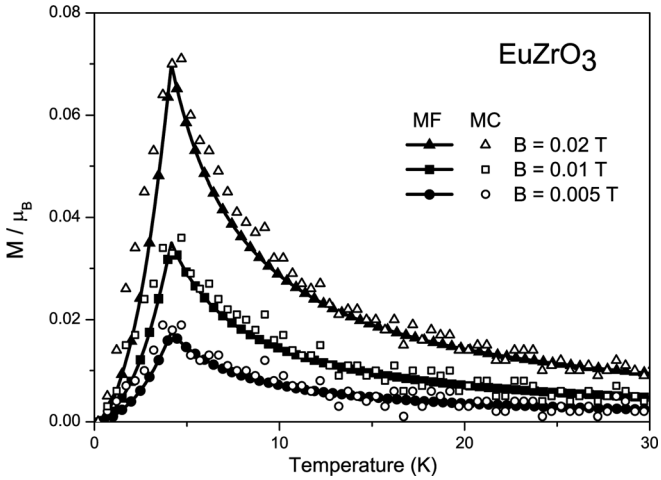

FIG. 2. Magnetization vs temperature in $EuZrO_3$ for applied magnetic fields $B = 0.005$, 0.01, and 0.02 T, using the mean field (solid curves) and Monte Carlo (open symbols) approaches.

versus T in Fig. 2, are, as expected, typical for an antiferromagnetic system when in the presence of an applied magnetic field. The magnetization increases with the temperature until around the Néel temperature and a small shift of the M peak occurs toward lower temperatures as the magnetic field is increased.

Figure 3 shows the temperature dependence of the magnetic susceptibility in $EuZrO_3$ under the external magnetic field, $B = 5 \times 10^{-3}$ T. The open circles represent the experimental data,[15] and the solid curve and triangles represent the theoretical results using mean field and Monte Carlo approaches, respectively. Good agreement between the experimental data and the theoretical results was obtained in both the antiferromagnetic and paramagnetic phases. It should be mentioned that the experimental data for the magnetic susceptibility were obtained in Ref. 15 for a polycrystalline $EuZrO_3$ sample and, therefore, the proper relation for the susceptibility calculation $\chi_P = (1/3)\chi_{\|} + (2/3)\chi_{\perp}$ was used, where $\chi_{\perp}$ is constant for temperatures below T_N, and is

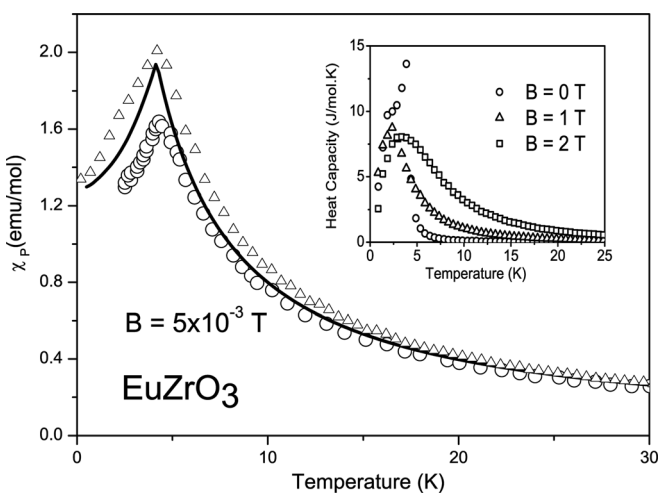

FIG. 3. Magnetic susceptibility vs temperature in $EuZrO_3$ at $B = 0.005$ T. Experimental data (circles), Monte Carlo simulation (triangles), and mean field calculation (solid curve). The inset shows the total heat capacity vs temperature from the Monte Carlo simulation, under $B = 0$, 1, and 2 T.

given by the value of the parallel susceptibility peak at T_N. For temperatures above T_N, $\chi_{\perp} = \chi_{\|}$, and $\chi_{\|} = M/B$ for the mean field approximation, and are given by relation (13), for the Monte Carlo simulations.

The magnetic field dependence of the magnetization in $EuZrO_3$ at T = 2 K is shown in Fig. 4(a). The full circles represent the experimental data;[15] the solid curve and triangles represent the theoretical results using mean field and Monte Carlo approaches, respectively. Both theoretical results are in good agreement with the experimental data, showing an abrupt change in the magnetization around $B = 1$ T, which can be ascribed to a spin flipping. Then, M gradually increases into a ferromagnetic arrangement when increasing B. For $B < 1$ T, the Monte Carlo simulation better reproduces the experimental data compared with the mean field calculation, which leads to smaller values of the magnetization. Figure 4(b) shows a comparison between the mean field approximation and the Monte Carlo simulation for the magnetic field dependence of the magnetization for several temperatures (T = 1, 2, and 3 K). Full and open symbols represent the results for the mean field and Monte Carlo, respectively. For both approaches one can conclude that the magnetization change shrinks and shifts to a lower magnetic field with increasing temperature. In the Monte Carlo simulation, the change in M around $B = 1$ T, for T = 2 K, is less abrupt than that observed using the mean field calculation. We attribute this difference to the loss of short range order interactions in the mean field approximation.

The temperature dependence of the isothermal entropy change, ΔS_T, is shown in Fig. 5 for magnetic field changes from 0 to 1 T and from 0 to 2 T. The full symbols represent the theoretical results from the mean field approximation and the open symbols represent the Monte Carlo simulation. It should be noted that the total entropy change is equal to the magnetic entropy change in the isothermal process, since we do not consider the magneto-elastic interaction where the lattice entropy may depend on the magnetic field and magnetization. For both mean field and Monte Carlo procedures, the $-\Delta S_T$ versus T is positive for the magnetic field change, $\Delta B : 0 \rightarrow 2\ T$, as expected for a normal ferromagnetic material. Alternatively, for the magnetic field change, $\Delta B : 0 \rightarrow 1\ T$, in both calculations, the inverse magnetocaloric is predicted in $EuZrO_3$. The inverse magnetocaloric effect is expected to occur in antiferromagnetic materials below the Néel temperature and can be physically explained. When an antiferromagnetic material is placed in a magnetic field and the temperature is increased, the spins localized in the sublattice oriented in the same direction of the applied field tend to increase at the expense of the opposite spin field sublattice. Therefore, the magnetization increases and the entropy decreases leading to negative values of $-\Delta S_T$ versus T below the Néel temperature. In the paramagnetic phase, the entropy always increases with temperature and $-\Delta S_T$ versus T is positive, as shown in Fig. 5. In general, the inverse magnetocaloric effect is expected to occur when the magnetization increases with temperature as stated by the Maxwell relation, which relates the field derivative of the entropy with the temperature derivative of the magnetization, i.e., the sign of the $-\Delta S_T$ versus T depends on the sign of the temperature

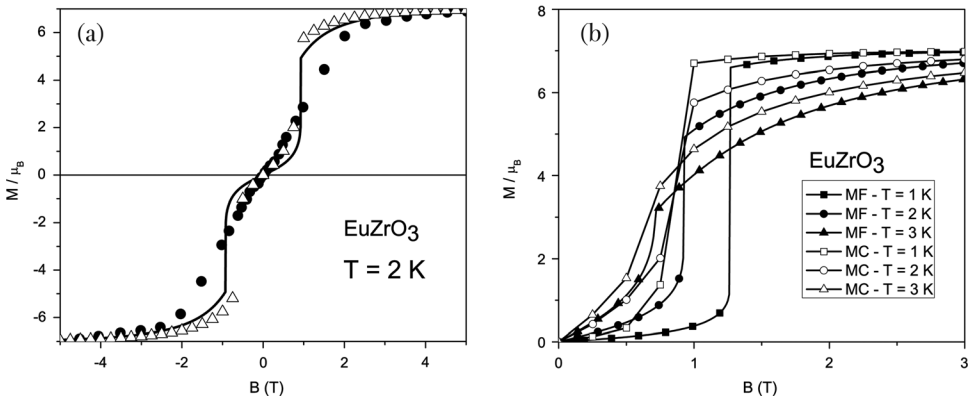

FIG. 4. (a) Magnetization vs applied magnetic field in $EuZrO_3$ at $T = 2$ K. Experimental data (full circles), mean field calculation (solid curve), and Monte Carlo simulation (open triangles). (b) Magnetization vs applied magnetic field in $EuZrO_3$ for several temperatures. Full symbols are for mean field (MF) and open symbols are for Monte Carlo (MC).

derivative of the magnetization. Above the Néel temperature, both mean field and Monte Carlo simulation predictions are in good agreement. Below the Néel temperature, in the MFA, the absolute peak value in $-\Delta S_T$ for the inverse magnetocaloric effect curve is higher than the Monte Carlo ones. For the curve of the direct magnetocaloric effect, $\Delta B : 0 \rightarrow 2\ T$, a different profile is observed, i.e., a concave increase occurs for the Monte Carlo prediction and a convex increase is predicted with the mean field approximation. Experimental results for $-\Delta S_T$ in $EuZrO_3$ are desired in order to verify the real profile below the Néel temperature and to perform further theoretical analysis. An interesting physical prediction in our calculation is the change from inverse to direct magnetocaloric effect that is observed between the two magnetic field changes, $\Delta B : 0 \rightarrow 2\ T$ and $\Delta B : 0 \rightarrow 1\ T$, which can be directly associated with the field induced transformation from an antiferromagnetic to a ferromagnetic arrangement as discussed above, experimentally observed in $EuZrO_3$, and shown in Fig. 4.

In order to calculate the adiabatic temperature change, ΔT_{ad}, the lattice entropy should be included and the Debye approximation was considered using relation (9). We did not find the Debye temperature for $EuZrO_3$ in the literature. Usually, the perovskite oxides have high Debye temperatures compared to the magnetic intermetallics. The most similar compounds we found were $CaZrO_3$ ($\Theta_D = 631$ K)[21] and $BaZrO_3$ ($\Theta_D = 525$ K).[22,23] Therefore, in order to perform the ΔT_{ad} calculation, we adopted the Debye temperature, $\Theta_D = 600$ K, for $EuZrO_3$. Figure 6 shows the total entropy versus T curves and the corresponding ΔT_{ad} calculated for $EuZrO_3$, with $B = 0$ T and $B = 2$ T. The solid curves represent the mean field calculations and the open triangles represent the Monte Carlo simulation. The total entropy curves using the MFA were calculated using relation (7) and the total entropy curves from the Monte Carlo simulation were calculated by proper integration of the heat capacity curves shown in the inset of Fig. 5, which were obtained from relation (12). The total entropy curves with B = 0 and B = 2 T (see Fig. 6), do not cross each other, and therefore ΔT_{ad} is always positive (a direct adiabatic magnetocaloric effect). Figure 7 shows the same physical quantities investigated under the B = 0 and B = 1 T. A crossing can be observed in the total entropy curves with B = 0 and B = 1 T, leading to the inverse adiabatic magnetocaloric effect ($\Delta T_{ad} < 0$) below $T \sim 4$ K. In this way, $EuZrO_3$ is predicted to heat up below $T \sim 4$ K under the magnetic field change, $\Delta B : 0 \rightarrow 2$ T, and to cool down under the magnetic field change, $\Delta B : 0 \rightarrow 1$ T.

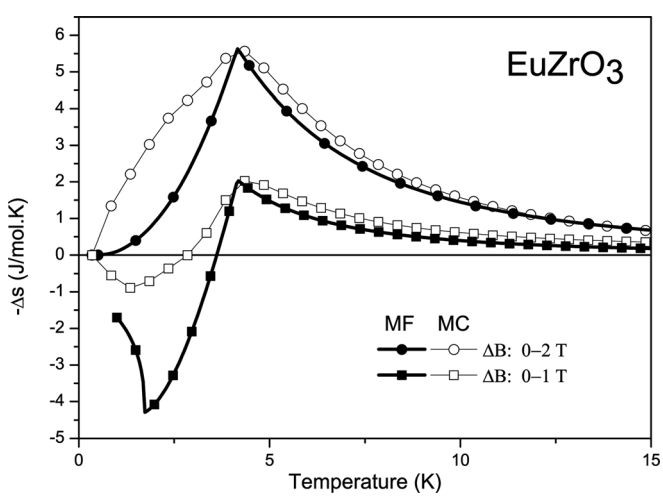

FIG. 5. ΔS_T vs temperature in $EuZrO_3$ for magnetic field changes from 0 to 1 T and from 0 to 2 T. Mean field calculation (full symbols) and Monte Carlo simulation (open symbols).

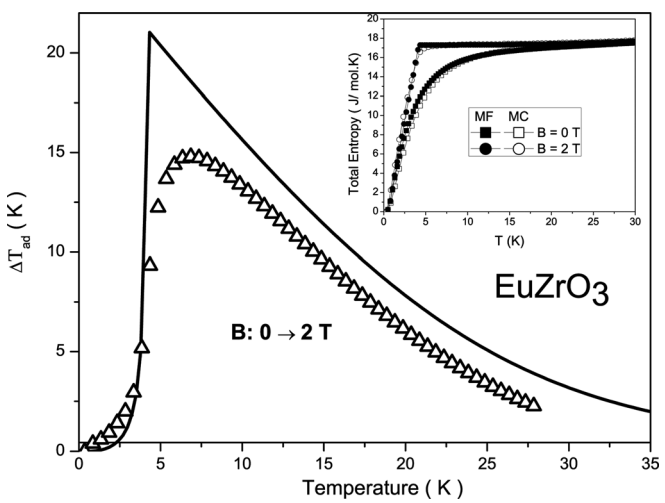

FIG. 6. Total entropy vs temperature in $EuZrO_3$ for magnetic fields $B = 0$ and 2 T (inset). Adiabatic temperature changes, ΔT_{ad}, upon magnetic field change from 0 to 2 T. Mean field calculation (solid lines) and Monte Carlo simulation (symbols).

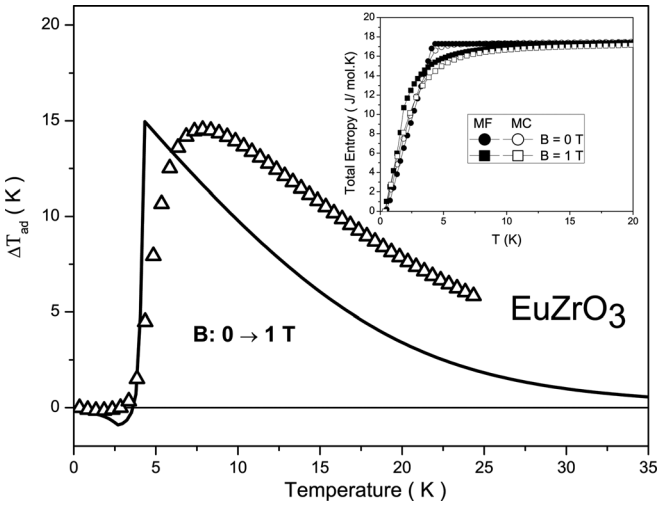

FIG. 7. Total entropy vs temperature in $EuZrO_3$ for magnetic fields $B = 0$ and 1 T (inset). Adiabatic temperature changes, ΔT_{ad}, upon magnetic field change from 0 to 1 T. Mean field calculation (solid curves) and Monte Carlo simulation (symbols).

IV. FINAL COMMENTS

The thermal and magnetic properties of the perovskite compound were theoretically investigated focusing on the magnetocaloric effect. Mean field calculations and Monte Carlo simulations were performed to deal with the proper magnetic Hamiltonian for $EuZrO_3$. The inverse and direct magnetocaloric effects were predicted to occur for magnetic field changes from 0 to 1 T and from 0 to 2 T, respectively. This anomalous magnetocaloric behavior in $EuZrO_3$ was ascribed to the change from antiferromagnetic to ferromagnetic arrangements induced by an applied magnetic field around $B = 1$ T for $T = 2$ K. The Monte Carlo simulation better reproduces the experimental M versus B data for $B < 1$ T. Different concavity profiles were predicted in ΔS_T versus T curves for a magnetic field change from 0 to 2 T by Monte Carlo and mean field calculations procedures. In the intermetallics, $GdNi_5$, the nature of the concavity in ΔS_T was associated with the density of the magnetic states at low temperature.[24] The predicted anomalous behavior in the magnetocaloric quantities and their profiles in $EuZrO_3$ requires further experimental investigation.

ACKNOWLEDGMENTS

We acknowledge financial support from CNPq–Conselho Nacional de Desenvolvimento Científico e Tecnológico–Brazil, FAPERJ–Fundação de Amparo à Pesquisa do Estado do Rio de Janeiro, CAPES–Coordenação de Aperfeiçoamento do Pessoal de Nível Superior, and FAPESP–Fundação de Amparo à Pesquisa do Estado de São Paulo.

[1]E. Warburg, Ann. Phys. **13**, 141 (1881).
[2]V. K. Pecharsky and K. A. Gschneidner, Jr., Phys. Rev. Lett. **78**, 4494 (1997).
[3]P. J. von Ranke, N. A. de Oliveira, and S. Gama, J. Magn. Magn. Mater. **277**, 78 (2004).
[4]N. A. de Oliveira and P. J. von Ranke, Phys. Rev. B **77**, 214439 (2008).
[5]P. J. von Ranke, N. A. de Oliveira, E. J. R. Plaza, V. S. R. de Sousa, B. P. Alho, A. Magnus G. Carvalho, S. Gama, and M. S. Reis, J. Appl. Phys. **104**, 093906 (2008).
[6]P. Sande, L. E. Hueso, D. R. Miguens, J. Rivas, F. Rivadulla, and M. A. Lopez-Quintela, Appl. Phys. Lett. **79**, 2040 (2001).
[7]H. Yamada and T. Goto, Physica B **346–347**, 104 (2004).
[8]E. P. Nobrega, N. A. de Oliveira, P. J. von Ranke, and A. Troper, Phys. Rev. B **74**, 144429 (2006).
[9]A. M. Tishin and Y. I. Spichkin, *The Magnetocaloric Effect and its Applications*, 1st ed. (Institute of Physics, Bristol, 2003).
[10]N. A. de Oliveira and P. J. von Ranke, Phys. Rep. **489**, 89 (2010).
[11]S. Sasaki, C. T. Prewitt, and R. C. Liebermann, Am. Mineral. **68**, 1189 (1983).
[12]M. D. Kuz'min and A. M. Tishin, J. Phys. D: Appl. Phys. **24**, 2039 (1991).
[13]H. Kimura, T. Numazawa, M. Sato, T. Ikeya, and T. Fukuda, J. Appl. Phys. **77**, 432 (1995).
[14]M.-H. Phan and S.-C. Yu, J. Magn. Magn. Mater. **308**, 325 (2007).
[15]Y. Zong, K. Fujita, H. Akamatsu, S. Murai, and K. Tanaka, J. Solid State Chem. **183**, 168 (2010).
[16]T. Kolodiazhnyi, K. Fujita, L. Wang, Y. Zong, K. Tanaka, Y. Sakka, and E. Takayama-Muromachi, Appl. Phys. Lett. **96**, 252901 (2010).
[17]J. E. Greedan, C.-L. Chien, and R. G. Johnston, J. Solid State Chem. **19**, 155 (1976).
[18]E. P. Nóbrega, N. A. de Oliveira, P. J. von Ranke, and A. Troper, Phys. Rev. B **72**, 134426 (2005).
[19]E. P. Nóbrega, N. A. de Oliveira, P. J. von Ranke, and A. Troper, J. Magn. Magn. Mater. **320**, e147 (2008).
[20]D. P. Landau and K. Binder, *A Guide to Monte Carlo Simulations in Statistical Physics* (Cambridge University Press, Cambridge, 2000).
[21]H. Yang, Y. Ohishi, K. Kurosaki, H. Muta, and S. Yamanaka, J. Alloys Compd. **504**, 201 (2010).
[22]R. Terki, G. Bertrand, H. Aourag, and C. Coddet, J. Alloys Compd. **456**, 508 (2008).
[23]D. Bagayoko, G. L. Zhao, J. D. Fan, and J. T. Wang, J. Phys. Condens. Matter, **10**, 5645 (1998).
[24]P. J. von Ranke, M. A. Mota, D. F. Grangeia, A. Magnus G. Carvalho, F. C. G. Gandra, A. A. Coelho, A. Caldas, N. A. de Oliveira, and S. Gama, Phys. Rev. B **70**, 134428 (2004).